EXPERIMENTAL STUDY ON TURBIDITY CURRENTS TRANSPORTING MICROPLASTICS IN DIFFERENT CANYON TOPOGRAPHIES

YANG LU [1], XIAOLEI LIU [2]

[1] *Shandong Provincial Key Laboratory of Marine Environment and Geological Engineering, Ocean University of China, China, luyang2017@163.com*

[2] *Shandong Provincial Key Laboratory of Marine Environment and Geological Engineering, Ocean University of China;*

Laboratory for Marine Geology, Qingdao Marine Science and Technology Center, China, xiaolei@ouc.edu.cn

Introduction

Nowadays, plastics or microplastics in the marine environment has gain lots of attention due to their harm to marine ecosystems and human health (Kane et al., 2019). Previous studies have focused more on the plastic distribution around the sea surface, but the physical process of transport and burial of plastics in the deep oceans remains unclear. Given that most of these plastics (probably 99%) are buried in the deep oceans and the turbidity currents are proposed to be the main carrier for plastic transport (Pohl et al., 2020), it is necessary to understand how the turbidity currents transport the plastics and make them buried in the seabed.

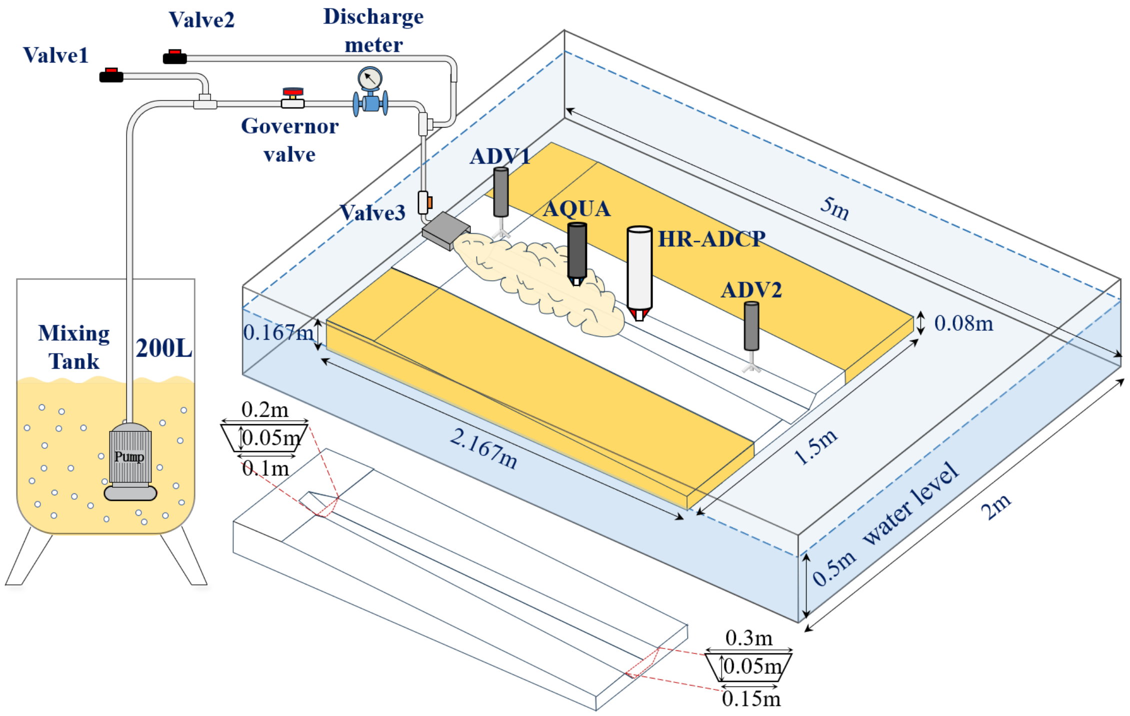

Figure 1. Experimental apparatus of turbidity currents transporting microplastics in the canyon topography

Methods

Based on the Froude scaling approach (Straub et al., 2008), we designed a series of experiments on turbidity currents transporting microplastics in different canyon topographies. The turbidity currents are composed of kaolin clay, quartz and fresh water, and the canyon topography is set to be straight or sinuous. These experiments were carried out in a water tank with high-resolution and high-frequency acoustic measuring instruments equipped (Figure 1), including the acoustic Doppler velocimeter (ADV), suspended sediment profiler (AQUA), and the high-resolution acoustic Doppler current profiler (HR-ADCP).

Results

The preservation rate of microplastics in canyons can reach up to 87.69%. Results show that the topography is an important factor affecting the deposition of microplastics, specifically, the canyon sinuosity increases the preservation rate. The preferential deposition zone of microplastics is located at the lee side of the wavy sediment deposits in the canyon head (Figure 2). Additionally, changes in flow rate and concentration of turbidity currents regulate the preservation rate and the distance between microplastic-enriched area and canyon head.

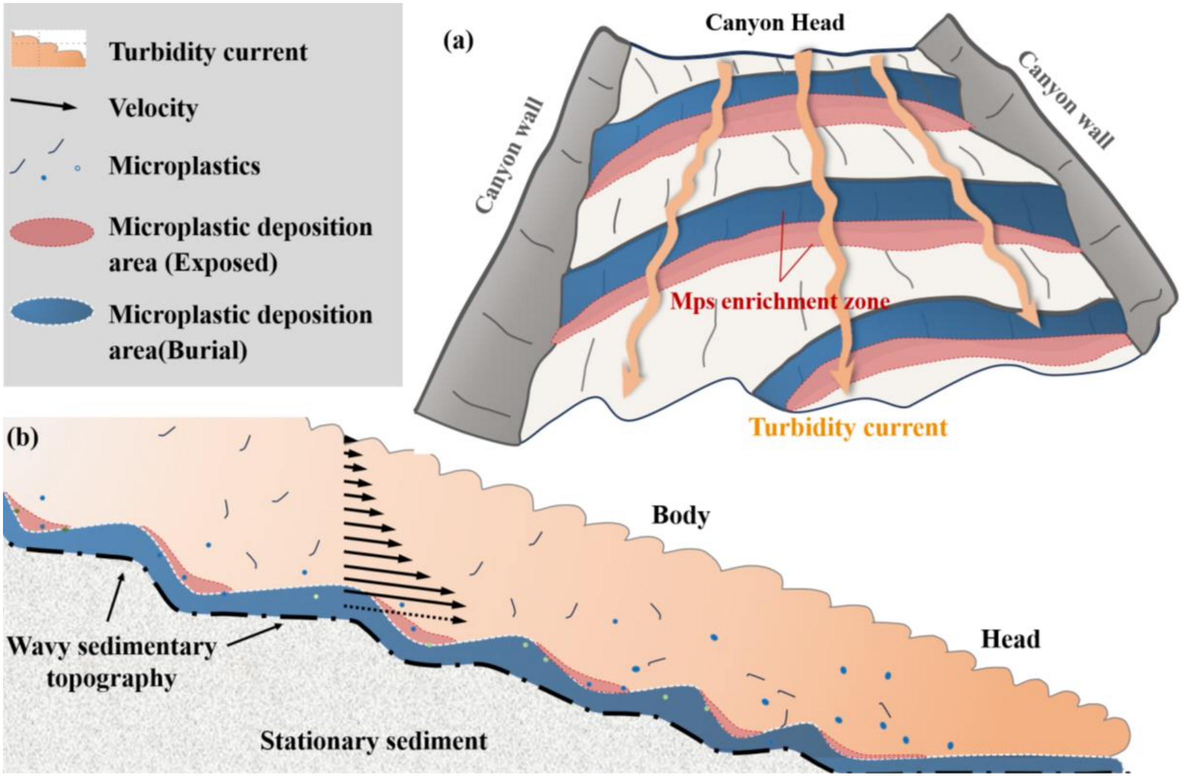

Figure 2. Schematic diagram showing the mechanism of microplastic deposition on the wavy deposits

Conclusion

This study adopts an experimental approach to investigate the migration and deposition characteristics of microplastics in different canyon topographies. The properties of turbidity currents and canyon sinuosity comprehensively determine the ultimate fate of microplastics transported in canyons. This study can provide valuable insights into evaluating the possible effects of plastics on marine environments and ecosystems.

References

Straub, K. M.; Mohrig, D.; McElroy, B.; Buttles, J.; Pirmez, C. Interactions between turbidity currents and topography in aggrading sinuous submarine channels: A laboratory study. *GSA Bulletin*, 2008, 120(3-4), 368-385.

Kane, I. A.; Clare, M. A. Dispersion, accumulation, and the ultimate fate of microplastics in deep-marine environments: A review and future directions. *Frontiers in Earth Science*, 2019, 7, 00080.

Pohl, F.; Eggenhuisen, J. T.; Kane, I. A.; Clare, M. A. Transport and burial of microplastics in deep-marine sediments by turbidity currents. *Environmental Science & Technology*, 2020, 54: 4180-4189.

MULTI-HAZARD ASSESSMENT OF SOIL EROSION AND LANDSLIDE SUSCEPTIBILITY IN THE DRAINAGE BASIN OF THE PINIOS DAM IN GREECE

MARIA MICHALOPOULOU[1], SPYRIDON LAINAS[1], NIKOLAOS DEPOUNTIS[1]

[1] *Department of Geology, Laboratory of Engineering Geology, University of Patras, 265 04 Patras, Greece*
maria_michalopoulou@ac.upatras.gr

Introduction

Soil erosion is a critical natural phenomenon that could be characterized as a hazard due to its varying intensity across different regions (Depountis et al., 2020), which frequently leads to surficial or shallow landslides, posing substantial risks to human lives, infrastructure, and the natural environment with substantial socio-economic impacts. In EU countries, 1 billion tons of soil are lost annually due to erosion, with Greece ranking among the top three Mediterranean countries, alongside Italy and Spain, exhibiting the highest recorded soil erosion rates (Panagos et al., 2020). Especially in Western Greece the phenomenon of erosion is more intense and for this reason the present research focuses on the southern part of the Pinios dam drainage basin, which is particularly vulnerable to soil erosion and landslides (Lainas et al., 2021; Michalopoulou et al., 2022). The steep terrain, the geological conditions, the poor soil cover, the intense rainfall patterns, as well as wildfires that have occurred during the previous decades, have significantly contributed to the area's increased susceptibility to soil erosion and landslides. Taking these factors into account, a modelling approach using the Revised Universal Soil Loss Equation (RUSLE) and the Landslide Susceptibility Index (LSI) was applied to identify areas prone to erosion and landslides within the study area. The aim of this study is to provide valuable insights into the spatial distribution and the severity of soil erosion and landslides by investigating their correlation and the combined effect of dominant causal factors that play a major role in their activation. Establishing a multi-hazard approach towards the identification of areas with the highest susceptibility can be considered a fundamental step in establishing mitigation strategies at local and regional levels.

Methods

This study focuses on two main hazards that prevail in the research area of the Pinios dam drainage basin, which are the soil erosion and landslide occurrence. To assess the soil erosion analysis, the RUSLE model was used by incorporating the parameters of rainfall-runoff erosivity, soil erodibility, slope length and steepness, land cover management, as well as support practices. The Rainfall-Runoff Erosivity Factor (R) was calculated based on the mean annual precipitation. The Soil Erodibility Factor (K) was assessed by using the methodology by Wischmeier and Smith (1978) in the prevailing geological formations and the Slope Length and Steepness Factor (LS) was estimated using the Calsite method and a DEM with 5m accuracy. The Cover Management Factor (C) was estimated using the Corine Land Cover (CLC) database (2018 version), and finally, the Support Practice Factor (P) was assigned a unity value because of the lack of available data on the management practices implemented in the study area. The multiplication of the above factors, using ArcGIS Pro v.3.3.1, led to the creation of an annual soil erosion map of the study area in tonnes/ha/year. The landslide susceptibility was estimated by applying the Frequency Ratio (FR) method. The FR is a statistical method that can been used to analyze the relationship between the distribution of landslides and contributing factors (geology, precipitation, slope and land-use). When the FR value is above unity it indicates a positive correlation between the landslide occurrence and the specific class of the contributing factor, suggesting higher landslide susceptibility. Based on the FR values for each category of the contributing factors, the LSI was calculated as the sum of the corresponding FR values.

Results

The results of this study demonstrate that areas with the highest erosion potential are predominantly located along the steep valley sides of the Pinios River and its tributaries. In terms of landslide susceptibility, areas most prone to landslides are characterized by slope angles between 15° and 45°, mean annual precipitation ranging from 600 to 1000 mm, geological conditions dominated by Pleio-Pleistocene sediments, and agricultural land primarily consisting of complex cultivation, along with agricultural land with areas of natural vegetation. The most prone to erosion areas were the ones where the soil erosion rate was higher than the mean value estimated by the RUSLE model. Similarly, the most prone to landslides areas were areas with LSI values higher than the mean LSI value. The identification of the areas prone to the examined hazards is showed in Figure 1.

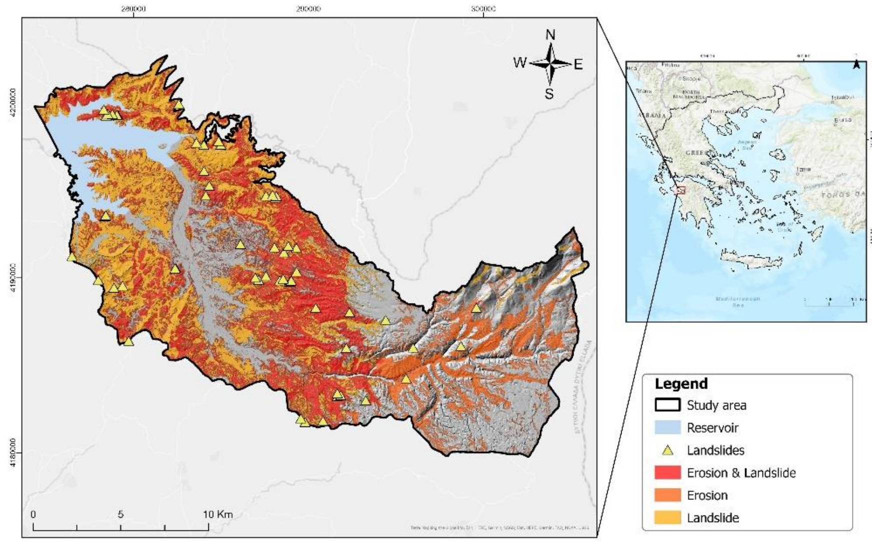

Figure 1. The multi-hazard map of the research area regarding to soil erosion and landslides.

Conclusions

This research method allowed to develop a multi-hazard map by integrating both soil erosion and landslide susceptibility. By utilizing GIS, regions with high erosion potential were superimposed with those highly susceptible to landslides. The percentage of the areas prone to soil erosion is equal to 33.94%, while the corresponding percentage regarding landslides is equal to 48.06%. The combined assessment of both hazards showed that the total percentage of the research area that can be affected by them is equal to 22.00%. Considering that under specific geological conditions soil erosion and shallow landslides are phenomena with similar generation patterns, combined triggering and effect, this approach has facilitated the identification of areas prone to soil erosion and landslide occurrence (multi-hazard approach) which is crucial for the implementation of suitable preventative measures and effective strategies by the state authorities, especially towards the assessment of the sustainability of the dam reservoir.

References

Depountis, N., Michalopoulou, M., Kavoura, K., Nikolakopoulos, K., & Sabatakakis, N. (2020). *Estimating soil erosion rate changes in areas affected by wildfires*. ISPRS International Journal of Geo-Information, 9(10), 562.

Lainas, S., Depountis, N., & Sabatakakis, N. (2021). *Preliminary Forecasting of Rainfall-Induced Shallow Landslides in the Wildfire Burned Areas of Western Greece*. Land, 10(8), 877.

Michalopoulou, M., Depountis, N., Nikolakopoulos, K., & Boumpoulis, V. (2022). *The significance of digital elevation models in the calculation of LS factor and soil erosion. Land*, 11(9), 1592.

Panagos, P.; Ballabio, C.; Poesen, J.; Lugato, E.; Scarpa, S.; Montanarella, L.; Borrelli, P. *A Soil Erosion Indicator for Supporting Agricultural, Environmental and Climate Policies in the European Union*. Remote Sens. 2020, 12, 1365.

Wischmeier, W.H.; Smith, D.D. *Predicting Rainfall Erosion Losses, a Guide to Conservation Planning; Agriculture Handbook No. 537*; US Department of Agriculture, Science and Education Administration: Washington, DC, USA, 1978.

DAMAGE EVOLUTION OF GRANITE-ENCASED- CONCRETE STRUCTURE UNDER STEPWISE CYCLIC TRIAXIAL LOADING

XIN YU [1], SHENGWEN QI [1], JOHN KEMENY [2], YUYE TAN [3], WEIDONG SONG [3], SONGFENG GUO [1], BOWEN ZHENG [1]

[1] *Institute of Geology and Geophysics, Chinese Academy of Sciences, Beijing, China, yuxin@mail.iggcas.ac.cn, qishengwen@mail.iggcas.ac.cn, guosongfeng@mail.iggcas.ac.cn, zhengbowen@mail.iggcas.ac.cn*

[2] *University of Arizone, Tucson, US, kemeny@arizone.edu*

[3] *University of Science and Techenology Beijing, Beijing, China, tanyuye@ustb.edu.cn, songwd@ustb.edu.cn*

Introduction

Rock-encased-backfill (RB) structures are common in underground mining engineering, for example in the cut-and- fill and stoping methods. To understand the effects of cyclic excavation and blasting activities on the damage of these RB structures, a series of triaxial stepwise-increasing-amplitude cyclic loading experiments was conducted with cylindrical RB specimens (rock on outside, backfill on inside) with different volume fractions of rock (VF = 0.48, 0.61, 0.73, and 0.84), confining pressures (0, 6, 9, and 12 MPa), and cyclic loading rates (200, 300, 400, and 500 N/s). The damage evolution and meso-crack formation during the cyclic process were analysed with results from stress-strain hysteresis loops, acoustic emission events, and post-failure X-ray 3D fracture morphology.

Methods

Cylindrical RB specimens were prepared to represent the underground structure between rock and backfill during the backfilling process. The rock used in this study was granite, the most important ore-bearing rock mass of the Shangshan Island Gold Mine located in Shandong province, China. The backfill consisted of tailings from the same mine, 52.4-grade cement, and distilled water. The physical and chemical properties of the tailings are detailed in Yu et al. (2021, 2024). The test process and experiment can be seen in Fig. 1.

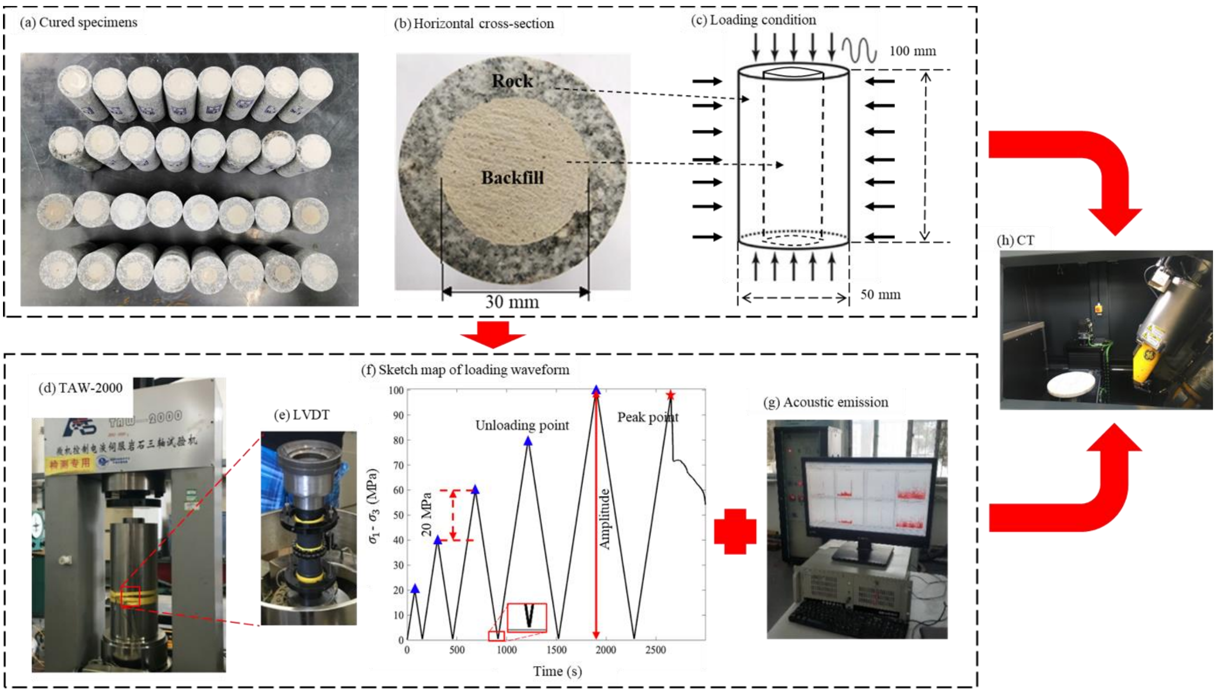

Figure 1. Rock-encased-backfill specimen (RB) and the experimental procedure.

Results

The results showed significant differences between cyclic and monotonic loadings of RB specimens, particularly with regard to the generation of shear microcracks, the development of stress memory and strain hardening, and the contact forces and associated friction that develops along the rock-backfill interface. One important finding is that as a function of the number of cycles, the elastic strain increases linearly and the dissipated energy increases exponentially. Also, compared with monotonic loading, the cyclic strain hardening characteristics are more sensitive to rising confining pressures during the initial compaction stage. Another finding is that compared with monotonic loading, more shear microcracks are generated during every reloading stage, but these microcracks tend to be dispersed and lessen the likelihood of large shear fracture formation. The transition from elastic to plastic behavior varies depending on the parameters of each test (confinement, volume fraction, and cyclic rate), and an interesting finding was that the transformation to plastic behavior is significantly lower under the conditions of 0.73 rock volume fraction, 400 N/s cyclic loading rate, and 9 MPa confinement (Figure 2). All the findings have important practical implications on the underground mining stability management.

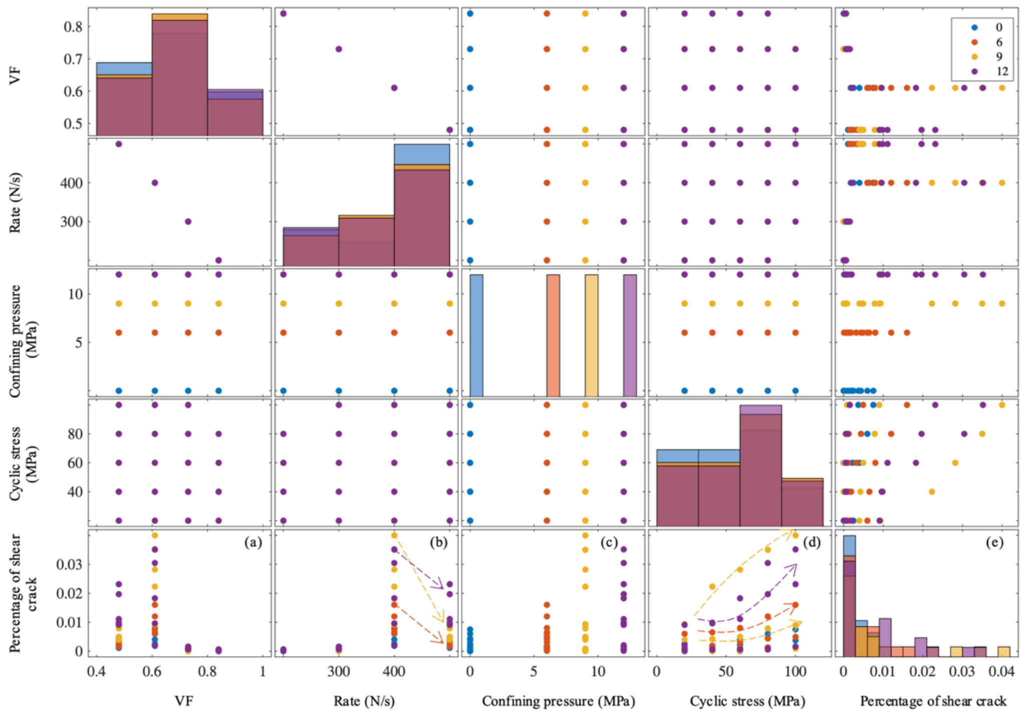

Figure 2. Relationship of VF, cyclic loading rate, confining pressure, cyclic stress, and percentage of shear crack.

Conclusion

The work presented here is unique and builds upon many studies of single material samples under monotonic and cyclic loadings, and bi-material samples under monotonic loading. As far as we know, this is the first comprehensive set of tests on rock encased backfill samples under cyclic loading.

References

Yu, X., J. Kemeny, J. Li, W. Song, and Y. Tan. 3D Observations of Fracturing in Rock-Backfill Composite Specimens Under Triaxial Loading, *Rock Mechanics & Rock Engineering*. 2021, 54(12), 6009-6022.

Yu, X., Y. Tan, W. Song, J. Kemeny, S. Qi, B. Zheng, and S. Guo. Damage evolution of rock-encased-backfill structure under stepwise cyclic triaxial loading, *Journal of Rock Mechanics and Geotechnical Engineering*. 2024.

HYDROGEOCHEMICAL MODELLING OF $CaCO_3$ SCALING FROM THE SERPENTINIZATION-DRIVEN HYPERALKALINE SRPINGS

VLADIMIR ŠARABA[1], TATJANA TRTIĆ-PETROVIĆ[2], TANJA PETROVIĆ PANTIĆ[3]

[1] *Laboratory of Physics, Vinča Institute of Nuclear Sciences, National Institute of the Republic of Serbia, University of Belgrade, Belgrade, Serbia, vladimir.saraba@vin.bg.ac.rs*

[2] *Laboratory of Physics, Vinča Institute of Nuclear Sciences, National Institute of the Republic of Serbia, University of Belgrade, Belgrade, Serbia, ttrtic@vin.bg.ac.rs*

[2] *Department of Geotechnics and Hydrogeology, Geological Survey of Serbia, Belgrade, Serbia, tanjapetrovic.hg@gmail.com*

Introduction

The serpentinization-driven hyperalkaline springs (HAS), with a pH value over 11.0 (Dragišić & Živanović, 2014) and mainly of Ca^{2+} - OH^{-} genetic type, are globally rare groundwater occurrences, with potential application in bottling, spa treatments and medical balneotherapy (Spahić et al., 2023). The carbonate minerals at HAS is typical of serpentinization in the worldwide peridotite massifs (Falk et al., 2016) and mineral scaling can affect serious operational problems in engineering geological investigations, such as membrane pores blockage and impairment of equipment functionality (Cao et al., 2022). This study is focused on the application of hydrogeochemical modelling to access the possibility of $CaCO_3$ scaling from the selected 4 HAS, designated as White Waters (WW-1, WW-2, WW-3 and WW-4, respectively), in the Mokra Gora area of the Zlatibor mountain of western Serbia belonging to the Dinaric ophiolite belt terrane in the central section of Balkan Peninsula (Nikić et al., 2013). The geographic position and geological composition of the wider research area is shown in Figure 1.

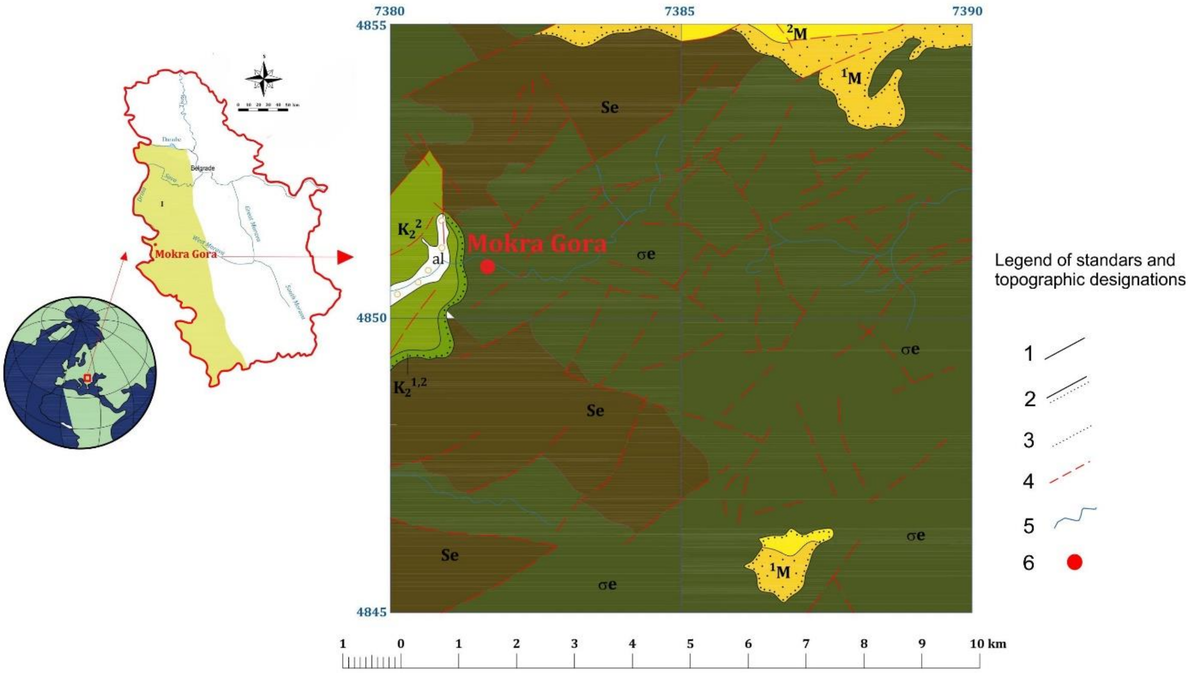

Figure 1. Schematic representation of geographic position and geological setting of the wider research area of Mokra Gora (Ciric et al., 2023; Mojsilović et al., 1978). Geological legend: I - Inner Dinarides of western Serbia; al – Alluvium; ^{2}M – Marlstones and dolomites; ^{1}M – Conglomerates and weakly cemented sandstones; K_2^{2} – Layered and sandy-marly limestones and marlstones; $K_2^{1,2}$ - Conglomerates, sandstones, claystones and oolitic iron ores; Se – Serpentinite; σe – Harzburgite. Legend of standard and topographic designations: : 1 - Normal boundary: determined; 2 - Erosional or tectonic-erosive boundary (determined); 3 – The boundary of gradual lithological transition; 4 – Fault: assumed; 5 – River; 6 – Mokra Gora research area.

The investigated occurrences originate from the wide Jurassic supra-custal on-land ophiolites, which are cumulates of mafic plus ultramfic origin and serpentinized peridotites (Spahić et al., 2023), and appear as linear ascending serpentinization-driven springs in the Kamišna River valley (Dragišić et al., 1999).

Methods

Hydrogeochemical modelling, using the program WATCH updated to version 2.4. website (Iceland Water Chemistry Group, 2010), was conducted to determine the saturation index (SI) for calcite in order to assess the possible precipitation of given mineral (SI>0) from the examined HAS. Additionally, we calculated the Langelier Saturation Index (LSI) to predict the $CaCO_3$ scaling (LSI>0) from the studied HAS. The SI and LSI were calculated based on the previously determined physico-chemical properties of the investigated HAS. The values of SI, LSI<0 show that saturation of $CaCO_3$ has not been reached from the examined HAS, while the SI, LSI≈0 indicates equilibrium between $CaCO_3$ and the investigated groundwaters.

Results and discussion

The WATCH program indicated the possible precipitation of calcite, taking into account that the positive SI values were linked with all examined HAS, i. e. 1.47 for WW-1, 1.42 for WW-2, 1.68 for WW-3 and 1.94 for WW-4 occurrence, respectively. This program is mostly used to explain the chemical composition of deep formation and geothermal fluids (Ma et al., 2023) and the HAS of Mokra Gora area discharges from the deep fractured zones (Dragišić et al., 1999). Also, the LSI confirmed the possible scaling of $CaCO_3$ from all investigated HAS, bearing in mind the LSI values of 1.3 for WW-1 and WW-3, 1.2 for WW-2 and 2.0 for WW-4 occurrence, respectively. The LSI is the most widely used index in the water field (Ozair et al., 2012), whereby this index was also applied to predict the $CaCO_3$ scaling from the selected HAS. The uptake of CO_2 in the zones of emergence of HAS contribute to the precipitation of $CaCO_3$, wherefore the HAS may have an environmental significance in terms of CO_2 storage (Spahić et al., 2023). Also, at high pH values, the CO_3^{2-} is dominant compared to HCO_3^- (Dragišić & Živanović, 2014), which is conducive to $CaCO_3$ scaling and aragonite is more commonly occurring as bottom deposits, while calcite as surface film (Spahić et al., 2023). Bearing in mind the foregoing, the main limitation of the program WATCH includes the impossibility of calculating the SI for aragonite, in order to access whether it can be precipitated from the investigated HAS, since it is possible to determine the SI only for minerals available with the WATCH program, such as calcite.

Conclusion

The results of the program WATCH and the LSI index consistently indicate the possibility of $CaCO_3$ scaling from the investigated 4 HAS, whereby hydrogeochemical modelling can be applied in engineering geological investigations for the prognosis of risk of the development of chemical clogging process of underground installations.

References

Cao, Z.; Hu, Y.; Zhao, H.; Cao, B.; Zhang, P.; Sulfate mineral scaling: From fundamental mechanisms to control strategies. *Water Research*, 2022, 222, 118945. https://doi.org/10.1016/j.watres.2022.118945

Ciric, M.; Šaraba, V.; Budin, C.; de Boer, T.; Nikodinovic-Runic, J.; Polyurethane-Degrading Potential of Alkaline Groundwater Bacteria. *Microbial Ecology*, 2024, 87(1), 21. https://doi.org/10.1007/s00248-023-02338-z

Dragišić, V.; Tišma, R..; Milenić, D.; Miladinović, B.; Potkonjak, B.; Špadijer, S.; Hiperalkalne mineralne vode Srbije. *In International Conference "Water for the 21st century*, 611-618; Water Technology and Sanitary Engineering Association, Belgrade, 1999.

Dragišić, V.; Živanović, V. *Opšta hidrogeologija*. University of Belgrade, Faculty of Mining and Geology, 2014.

Falk, E. S.; Guo, W.; Paukert, A. N.; Matter, J. M.; Mervine, E. M.; Kelemen, P. B. Controls on the stable isotope compositions of travertine from hyperalkaline springs in Oman: Insights from clumped isotope measurements. *Geochimica et Cosmochimica Acta*, 2016, 192, 1-28.

Iceland Water Chemistry Group. *The chemical speciation program WATCH, version 2.4. website*. ÍSOR - Iceland GeoSurvey, Reykjavik, 2010. https://en.isor.is/software/

Ma, S.; Yang, Y.; Lei, X.; Yue, B. Water scaling predication for typical sandstone geothermal reservoirs in the Xi'an Depression. *Energy Geoscience*, 2023, 100182. https://doi.org/10.1016/j.engeos.2023.100182

Mojsilović, S.; Baklaić, D.; Đoković, I.; *Geological map of Serbia 1:100000 – Titovo Užice*. Belgrade: Federal Geological Society, 1978. Available from: https://geoliss.mre.gov.rs/prez/OGK/RasterSrbija/OGKWebOrig/listovi.php?karta=Titovo_Uzice

Nikić, Z.; Sreckovic-Batocanin, D.; Burazer, M.; Ristic, R.; Papic, P.; Nikolic, V. A conceptual model of mildly alkaline water discharging from the Zlatibor ultramafic massif, western Serbia. *Hydrogeology Journal*, 2013, 21(5), 1147-1163. 10.1007/s10040-013-0983-2

Ozair, G. An overview of calcium carbonate saturation indices as a criterion to protect desalinated water transmission lines from deterioration. *Nature, Environment and Pollution Technology*, 2012, 11(2), 203-212. ISSN: 0972-6268

Spahić, D.; Nikić, Z.; Mukherjee, S.; Dokmanović, P. Discovery of hyperalkaline waters in the ophiolites of western Serbia: Environmental considerations for carbon capture and sequestration. *Geoenergy Science and Engineering*. 2023, 212319. https://doi.org/10.1016/j.geoen.2023.212319

INVESTIGATION OF THE ABSORBING PROPERTIES OF MODIFIED SANDY SOIL TO CREATE A GEOCHEMICAL BARRIER FOR STORAGE LANDFILLS MUNICIPAL SOLID WASTE

ALEXANDRA KOVALEVSKAYA [1], TATYANA MALIKOVA [2], IRINA RODKINA [3]

[1] *Lomonosov Moscow State University (MSU), Russian Federation, alexa.kovalevskaya@mail.ru*

[2] *Lomonosov Moscow State University (MSU), Russian Federation, malikovatv@my.msu.ru*

[3] *Lomonosov Moscow State University (MSU), Russian Federation, irina-rodkina2007@yandex.ru*

Introduction

Lead compounds may be among the hazardous components of municipal waste. Clay soils and organic substances have the best absorption capacity in relation to Pb, while sandy soils are practically unable to absorb it. Therefore, the development of a technique for creating a geochemical barrier against lead based on modified sandy soil is promising.

The aim of the work is to study the absorption capacity of sandy soils with the addition of a clay substance and an organic binder (starch) in relation to lead. During the work, the pH and Eh of the selected filtrate were also measured to identify patterns between the values obtained and the amount of lead absorbed by the soil.

Methods

To study the absorbing properties of the modified sandy soil, a model soil was created based on Lyubertsy sand J_3v_2 (the fraction content of 0.5-0.25 mm is 50%, 0.25-0.10 mm - 48%, 0.10-0.05 mm - 2%), kilic clay and organic binder (starch) in a ratio of 10:1:1. The study was conducted by dynamic filtering. A solution of $Pb(NO_3)_2$ lead nitrate with a concentration of Pb 1.25 g/l was passed through a 10 cm thick model soil in the filtration column. The filtrate was sampled in 100 ml every 2 hours and 48 minutes. For the accuracy of the obtained values, tests were carried out on three samples.

The determination of pH and Eh solutions was carried out potentiometrically on the pH-150 device in accordance with GOST R 51232-98: reference electrode EVP-1M4, measuring electrode ESL-45-11, the steepness of the electrode function 58.25.

The zero charge point of the soil pH_{ZPC} – is the pH value at which the total charge of the surface of the soil particles is zero. In this work, pH_{ZPC} was determined for modified sandy soil both before and after the filtration process to compare the pH_{ZPC} values before and after lead ion sorption. The acid-base method was used to determine the pH_{ZPC} value titration of soil against the background of electrolyte solutions of different concentrations, described by T.A. Sokolova and S.J. Trofimov. HNO_3 acid and KOH alkali were used as titrants, and NaCl solutions with concentrations of 0.5 M, 0.1 M and 0.01 M were used as an electrolyte.

The cation exchange capacity of the soil was determined for model soil (sand, clay, starch) and for sand modified only with kilic clay. The determination was carried out according to the method described by E.V. Arinushkina, based on saturation of the soil with sodium ion, followed by its determination by the gypsum method.

The concentration of lead in solutions was determined using the Quantum Z.ETA atomic absorption spectrometer, manufactured by NPO KORTEK, Moscow. The method of atomic absorption spectrometry (AAS) is based on the phenomenon of resonant absorption of light by free atoms (atomic vapor) of the element being determined.

Results

Based on the measured pH values of the filtrate, a relationship between the pH and the amount of filtrate selected was revealed. After a certain amount of time, the pH of the filtrate decreases from 7-8 to 5-6 units, which corresponds to the pH of the initial solution $Pb(NO_3)_2$, which indicates the completion of the

Pb absorption process by the soil. There was no correlation between the Eh values of the filtrate and its selected amount, which is probably due to the activity of living organisms trapped on the ground or in the filtration column.

The pH_{ZPC} values of 8.5 before absorption and 6.25 units after absorption correspond to the measured pH values of the filtrate and the general behavior of the soil during Pb absorption.

The measurement of soil CEC showed that the absorption of lead by the model soil does not depend on its CEC value (0.07 mg-eq/100 g for the entire model soil and model soil excluding starch), therefore, lead sorption does not occur in the exchange complex of the soil, but in more durable centers.

According to the results of measuring the concentration of Pb absorbed by the model soil, an absorption capacity value of 1.96 mg/g was obtained. At the same time, the created soil with a capacity of 10 cm retained Pb with a concentration of 1.25 g/l for 35.5 hours. The maximum amount of lead absorbed by clay and starch is 11.76 mg/g, which is much less than the values obtained by studying the absorption capacity of similar soils under static sorption conditions (on average 48.24 mg/g).

Conclusion

Thus, in this work, the absorption capacity of sandy soil modified with clay soil (montmorillonite) and organic binder (starch) in relation to lead was studied. A relationship was revealed between the pH value of the solution and the amount of absorbed lead under dynamic sorption conditions (absorption of Pb ions by the soil leads to a change in the pH of the filtrate). Determination of the Eh values of the filtrate showed that the Eh value is probably influenced by living organisms. The obtained pH_{ZPC} values satisfy the general pattern of pH solution behavior. According to the measurement of the cation exchange capacity, it was found that the absorption of lead cations does not depend on the value of the soil cation exchange capacity (0.072 mg-eq/100g for a mixture of sandy and clay soil and 0.069 mg-eq/100g for a mixture of sandy soil, clay soil and starch), therefore, the absorption of lead occurs with the formation of more durable complexes. The maximum amount of lead absorbed by such a soil at an initial concentration of lead in a solution of 1.25 g/l is 1.96 mg/g. The maximum amount of absorbed lead without taking into account the mass of sand (absorption by clay and starch) is 11.76 mg/g, which is much less than the values obtained by studying the absorption capacity of similar soils under static sorption conditions (on average 48.24 mg/g according to A.I. Kovalevskaya).

References

Arinushkina E.V. Manual on chemical analysis of soils. Moscow: MSU, 1971.

Kovalevskaya A.I. Creation of sorption barriers against lead on the basis of clay soils modified with organic binders: abstracts of the international conference «Lomonosov-2022», section «Ecological geology». – M., 2022.

Sokolova T.A., Trofimov S.J. Sorption properties of soils. Adsorption. Cationic exchange. Tula: Vulture and K, 2009.

DISTRICT-SCALE SEASONAL UNDERGROUND THERMAL ENERGY STORAGE: CHALLENGES AND OPPORTUNITIES IN THE CZECH REPUBLIC

GIANVITO SCARINGI[1], JAN JERMAN[1], TOMÁŠ KADLÍČEK[1], DAVID MAŠÍN[1], JAN NAJSER[1], JAKUB ROHÁČ[1]

[1] *Institute of Hydrogeology, Engineering Geology and Applied Geophysics, Faculty of Science, Charles University, Czech Republic, gianvito.scaringi@natur.cuni.cz*

Introduction and motivation

Energy geostructures (EGS) and shallow underground thermal energy storage (UTES) systems are receiving considerable attention from the research community and policymakers thanks to potential energy savings and the consequent reduction in energy expenditures and carbon emissions. The feasibility, design, and challenges related to UTES systems, in combination with EGS but also independent from them, are thus being explored extensively (Loveridge et al., 2020). UTES systems can mitigate the high temporal variability of renewable energy sources (RES), such as photovoltaics, solar thermal, and wind energy, which are affected by seasonality and local weather conditions (Lyden et al., 2022). In fact, as far as non-industrial consumption is concerned, over half of the energy demand is used for indoor heating and climatisation (Connolly, 2017). However, a fundamental offset exists between the time functions of energy production from RES and consumption (Fig. 1). This creates imbalances in the energy grid, with overproduction during daytime in summer months and increased needs in wintertime, resulting in high and volatile prices of electricity.

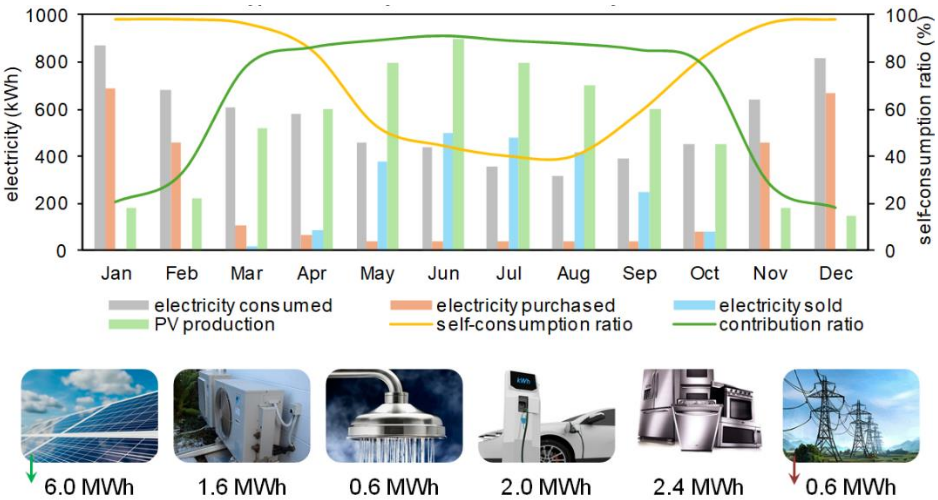

Figure 1. Typical electricity balance for a new family house in the Czech Republic.

UTES can mitigate this imbalance by storing excess energy in the form of heat underground (Yang et al., 2021) and subsequently retrieving it when it is needed, with considerable efficiency (Zymnis & Whittle, 2014). In the urban environment, with possible constraints in terms of available space, the spatial domain of UTES may intersect the areas of influence of building foundations and other underground infrastructures. This occurrence can also be intentional when foundations are themselves equipped with heat exchangers, such as in EGS. This specific design can be economically advantageous thanks to the double function (static and thermal) absolved by the structural elements. However, it also brings challenges as it triggers a coupled THM response in the ground-structure interaction. Further challenges relate to the upscaling of the design to serve not a single building but an entire district, where the energy needs and productions of the individual buildings (not only residential) are combined, with increased efficiency. While EGS with UTES are being studied extensively in other European countries (Aresti et al., 2024), the Czech Republic has been lagging behind. Here, no implementations of EGS with UTES exist, neither at the building nor at the district level. Besides regulatory complications, this stems from a lack of knowledge of the multiphysical long-term THM ground response to cyclic thermal loading, as well as from an insufficient understanding of the interaction with other RES and the associated challenges. Thanks to a grant we received from the Czech Ministry of Education, Youth and Sport (INTER-EXCELLENCE II programme, INTER-COST sub-programme, project no. LUC24143), we are taking the opportunity to realign ourselves to the international community and increase our readiness for the domestic adoption of these technologies. Our medium-term goal is to become a national reference and attract funding for applied research towards practical implementation.

Methods and Expected Outcomes

We aim to exploit our expertise in THM experiments and modelling and combine it with thermodynamic-based, multi-scale, and time-dependent knowledge of soil behaviour to enhance our understanding of the ground response through targeted experiments and the development of a modelling framework for UTES. In particular, we plan to incorporate a micro-structural representation of soil behaviour into a double-scale hypoplastic framework (Mašín, 2017) and introduce time- and rate-dependent formulations (Jerman & Mašín, 2020) of constitutive equations describing experimentally observed responses, such as thermal creep and plastic strain accumulation under cyclic loading (Pico & Mašín, 2024). Based on the developed framework, we will produce numerical implementations, which we will calibrate according to realistic boundary conditions determined from building practices, soil types, and climate scenarios in the Czech Republic. We will optimise these implementations to produce a numerical proof-of-concept of district-scale UTES, which will be the basis for follow-up applied research in cooperation with the industry.

Conclusion

Energy geostructures and underground thermal energy storage systems pose considerable engineering geological challenges and motivate substantial research. However, the Czech Republic has been lagging behind in the development of such solutions. We aim to exploit the opportunity of a newly funded project to bring advancements and make our country competitive in the implementation of solutions that considerably increase the usability of renewable energy and reduce the carbon footprint of buildings.

References

Aresti, L., et al. (2024). Energy Geo-structures: a review of their integration with other sources and its limitations. *Renewable Energy*, 230, 120835.

Connolly, D. (2017). Heat Roadmap Europe: Quantitative comparison between the electricity, heating, and cooling sectors for different European countries. *Energy*, 139, 580–593.

Jerman, J., Mašín, D. (2020). Hypoplastic and viscohypoplastic models for soft clays with strength anisotropy. *Int. Journal for Numerical and Analytical Methods in Geomechanics*, 44(10), 1396-1416.

Loveridge, F., McCartney, J.S., Narsilio, G.A., Sanchez, M. (2020). Energy geostructures: A review of analysis approaches, in situ testing and model scale experiments. *Geomechanics for Energy and the Environment*, 22, 100173.

Lyden, A., Brown, C.S., Kolo, I., Falcone, G., Friedrich, D. (2022). Seasonal thermal energy storage in smart energy systems: District-level applications and modelling approaches. *Renewable and Sustainable Energy Reviews*, 167, 112760.

Mašín, D. (2017). Coupled thermohydromechanical double-structure model for expansive soils. *Journal of Engineering Mechanics*, 143(9), 04017067.

Pico, M., Mašín, D. (2024). Coupled thermo-hydro-mechanical hypoplastic model for partially saturated fine-grained soils under monotonic and cyclic loading. *Computers and Geotechnics*, 172, 106447.

Yang, T., Liu, W., Kramer, G.J., Sun, Q. (2021). Seasonal thermal energy storage: A techno-economic literature review. *Renewable and Sustainable Energy Reviews*, 139, 110732.

Zymnis, D.M., Whittle, A.J. (2014). Numerical Simulation of a Shallow Geothermal Heating/Cooling System. Proceedings of the Geo-Congress 2014, pp. 2767–2776.